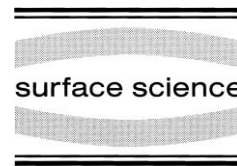




ELSEVIER

Surface Science 415 (1998) L1074–L1078



Surface Science Letters

Oscillatory relaxation of Al(110) reinvestigated by using medium-energy ion scattering

B.W. Busch, T. Gustafsson *

Department of Physics and Astronomy, and Laboratory for Surface Modification, Rutgers University, P.O. Box 849, Piscataway, NJ 08855-0849, USA

Received 25 June 1998; accepted for publication 24 July 1998

Abstract

Medium-energy ion scattering (MEIS) has been used to investigate the room-temperature structure of clean Al(110). The motivation for this work was the presence of a significant discrepancy between two previous independent low-energy electron diffraction results concerning the sign of the third-to-fourth layer relaxation. We find a damped oscillatory contraction–expansion for the first three interlayer spacings. The relaxation results are (in percent change from the bulk interlayer spacing): $\Delta d_{12} = -8.5 \pm 1.0\%$, $\Delta d_{23} = +4.8 \pm 1.2\%$ and $\Delta d_{34} = -3.9 \pm 1.4\%$. These results are compared with other theoretical and experimental values. © 1998 Elsevier Science B.V. All rights reserved.

Keywords: Aluminum; Low-index single-crystal surfaces; Medium-energy ion scattering (MEIS); Surface relaxation and reconstruction

Multilayer relaxation on clean metallic surfaces has been extensively studied both experimentally and theoretically. It has become quite clear that the changes in atomic coordination and electronic density, associated with the formation of the surface, lead to changes in the interlayer spacings. In particular, the open fcc(110) surfaces show a very strong effect. With the development of theories capable of treating the coupled system of ions and conduction electrons self-consistently, the agreement between experiment and theory for multilayer relaxations on metallic surfaces has improved remarkably, and in many cases may be considered quite good. Table 1 shows a compila-

tion of several experimental [1–3] and theoretical [4–10] results on the interlayer spacings of Al(110). As seen there, the various experimental results agree quite well for the first two interlayer relaxations. However, a notable discrepancy between two previous low-energy electron diffraction (LEED) results [1,2] arose concerning the sign of the third-to-fourth layer spacing. This problem is addressed below with medium-energy ion scattering (MEIS), and evidence is presented to support a significant contraction of the third-to-fourth layer spacing. The reason for this discrepancy is not known, but some possibilities are discussed.

Medium-energy ion scattering, with channeling and blocking, is a powerful method for determination of the structural and vibrational parameters

* Corresponding author. Fax: (+1) 732 445 4991; e-mail: gustaf@physics.rutgers.edu

Table 1

Values of the interlayer relaxations (in percentage change from bulk value, with negative numbers indicating a contraction) for several experimental and theoretical studies. For the two early LEED studies and the present MEIS results, values for the first-to-third, second-to-fourth and the sum of these are also shown

Experiment/Theory	Δd_{12}	Δd_{23}	Δd_{34}	Δd_{13}	Δd_{24}	$\Delta d_{13} + \Delta d_{24}$
LEED [1]	−8.6	+5.0	−1.6	−1.8	+1.7	−0.1
LEED [2]	−8.5	+5.5	+2.2	−1.5	+3.9	+2.4
LEED [3]	−7.1	+5.3	−3.3			
MEIS [this work]	−8.5	+4.8	−3.9	−1.9	+0.5	−1.4
Total energy calc. [4]	−10.0	+4.0	−3.0			
Total energy calc. [5]	−6.8	+3.5	−2.0			
Total energy calc. [6]	−5.35	+1.15	−3.04			
EAM [7]	−10.47	+3.64	−2.93			
EAM [8]	−10.4	+3.14	−2.75			
eDFT MD [9,10]	−7.3	+4.5	−2.0			

of a crystalline surface [11–13]. When incoming ions (e.g., 40–200 keV protons) are incident upon a crystalline surface along a major crystallographic direction or row of atoms, they are “channeled” into the solid. The deflection of the ions by the first atoms along a row causes the formation of a “shadow cone”, greatly reducing the chance of backscattering from successive atoms along the row. As ions travel through the solid, they continuously lose energy because of electronic stopping. Hence, the energy of an emerging backscattered proton is directly related to the depth of the scattering event. This effect, combined with channeling, gives rise to an energy distribution of the scattered particles that exhibits a “surface peak” at an energy that depends only on the scattering angle (angle away from the incident ion direction) and the masses of the projectile and target. Thermal displacements and reconstructions directly affect this process because they make channeling less perfect, and more ions are backscattered from the surface region. The area of the surface peak also depends on the direction in which the scattered ions are going. Ions exiting the crystal may be deflected by other atoms, “blocking”, resulting in a non-monotonic scattering angle dependence of the surface peak area. The position of such “blocking dips” provides a sensitive measure of surface-atom displacements. A shift in the position of a blocking dip away from the bulk crystal blocking direction is a direct indication of layer relaxation. Accurate determina-

tion of structural parameters (atomic locations and vibrational amplitudes) is accomplished by comparing the angular scattering intensity with Monte Carlo computer simulations [14,15] for trial structures. Structural and vibrational parameters in the simulations are varied until a good fit to the angular scattering intensity is achieved, as determined by an *R*-factor analysis [16].

Since scattering cross-sections are known accurately for the energy range used (Coulomb scattering with manageable screening), the area of the surface peak may be converted or “normalized” into visible atoms per row or, alternatively, into visible layers. We determine the normalization factors in the experiment, such as the detector solid angle and the fraction of the incident beam intercepted to measure the ion dose, by calibration with a Pt/Si high-energy ion scattering standard. The fraction of backscattered ions that are neutralized, and therefore cannot be detected by the electrostatic analyzer, is also accounted for.

Our ion scattering experiments were carried out with a 40.8 keV proton beam. The surface sensitivity of the MEIS technique is derived from the channeling effect, in which surface atoms deflect the incoming ions away from deeper atoms. An important parameter is the shadow cone radius [11,12]. This is the closest distance ions may approach the second atom along a row in a perfect static crystal. For effective channeling, and hence good surface sensitivity, the shadow cone radius should be substantially larger than the vibrational

amplitudes perpendicular to the rows of atoms. This parameter is proportional to the square root of the target atomic number, and inversely proportional to the square root of the beam energy. For aluminum, which is an element with a relatively low atomic number, use of incident protons with energy below ~ 50 keV gives good surface sensitivity. In this case, the shadow cone radius is approximately twice the bulk one-dimensional root-mean-square vibrational amplitude. We can measure the energy distribution of backscattered ions simultaneously over a 13° range in the scattering plane by using a high-resolution electrostatic analyzer in conjunction with micro-channel plates and a two-dimensional position-sensitive detector [17]. The system energy and angular resolutions for ~ 40 keV protons are ~ 48 eV and $\sim 0.1^\circ$, respectively.

The sample was prepared by standard sputtering and annealing cycles until a sharp (1×1) LEED pattern appeared. The base pressure of the ultra-high vacuum chamber was 2×10^{-10} Torr. Sample cleanliness could be monitored directly by MEIS backscattering. Oxygen impurities on the surface gave the most trouble. In a low scattering angle (high cross-section) configuration, the sensitivity of MEIS to oxygen is ~ 0.03 ML. This amount of oxygen was not detectable on the surface for approximately 5 h after cleaning. Data collection was kept within 2 h of cleaning.

Fig. 1a shows a top view of the Al(110) surface, and the two scattering planes (perpendicular to the surface) used in this experiment. For each plane, there are two inequivalent planes of atoms. One contains atoms in odd-numbered layers, while the other contains atoms in even-numbered layers. Both the first and second layers of the crystal are obviously visible to the incoming ion beam. Fig. 1b shows a side view of the $\{100\}$ scattering plane. The two inequivalent planes are distinguished in the figure by shading. The $\{110\}$ scattering configuration is very similar. With the aid of Fig. 1, it can be seen that shifts in the angular positions of blocking yields in the $\{100\}$ and $\{110\}$ planes are indicative of first-to-third and second-to-fourth interlayer relaxations. These parameters are denoted d_{13} and d_{24} , respectively. However, the detailed shape of the blocking yields contains

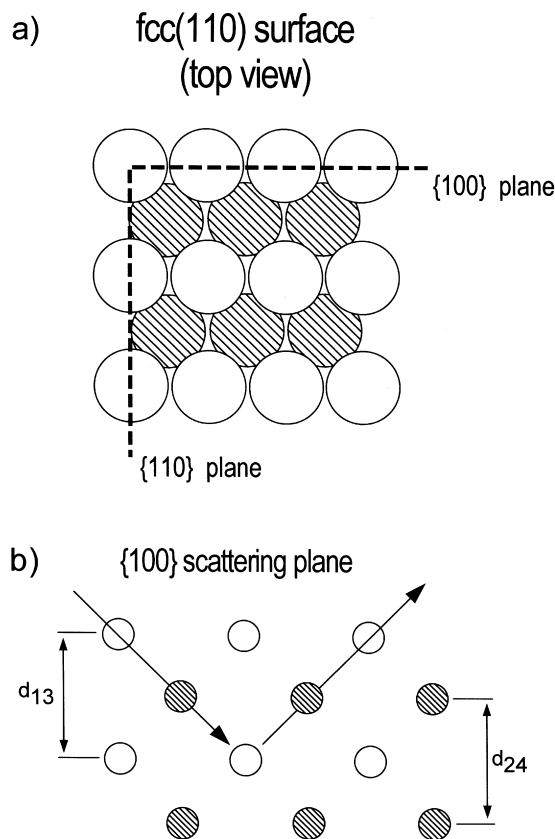


Fig. 1. (a) Top view of the Al(110) surface showing the two scattering planes (perpendicular to the surface) used for this work. Second-layer atoms are shaded. If the incident ion beam lies in either one of these planes, then both the first- and second-layer atoms are visible to the ion beam. (b) Side view of the $\{100\}$ scattering plane showing the two inequivalent planes (distinguished by shading), and the channeling and blocking directions. Angular scattering spectra in these planes are mostly sensitive to changes in d_{13} and d_{24} , indicated in the figure. The configuration in the $\{110\}$ plane is very similar.

information on all near-surface interlayer spacings. Therefore, ion-scattering simulations were carried out by relaxing the first three interlayer spacings simultaneously. The effect of including d_{45} in the analysis was negligible. An iterative approach was used between varying layer spacings and vibrational amplitudes. The various vibrational components in the first two layers were varied independently with the bulk amplitude fixed at the Debye result [18]. Our best-fit solution was found by

minimizing the sum of the R -factors [16] from the various scattering configurations.

The LEED results of Noonan and Davis [2] and Andersen et al. [1] disagree primarily on the value of d_{34} . Since the other layer spacings are in agreement, the discrepancy in d_{34} can be viewed as a discrepancy in d_{24} or in $d_{13} + d_{24}$. Recall that the positions of the blocking dips in the MEIS angular yields from the $\{100\}$ and $\{110\}$ scattering planes are equally sensitive to d_{13} and d_{24} , since both the first two layers are visible to the incident ion beam. This means that the angular position of the blocking dips in the $\{100\}$ and $\{110\}$ scattering planes are a qualitative measure of the total relaxation of d_{13} and d_{24} (last column of Table 1). With this fact, MEIS blocking dips from these two scattering planes provide a test of the two LEED structures. Fig. 2 shows the scattering data from the $\{100\}$ and $\{110\}$ scattering planes. Plotted with the data are the simulation results using our best-fit solution, as well as the simulation results using the structures from the two earlier LEED results. Vertical lines indicate the blocking dip positions for a bulk terminated surface. Use of $\sim 2\%$ expansion in d_{34} (Noonan and Davis structure) leads to a large value of $\Delta d_{13} + \Delta d_{24}$ which is incompatible with the data since it gives a visible shift in the blocking dip to *higher* scattering angles. Detailed structural results, including the first three interlayer spacings, come from simulations of the entire blocking yield in both scattering configurations. The optimum structure was determined from an R -factor analysis [16]. The best fit is obtained with a significant contraction of d_{34} . From this, and a simple inspection of Fig. 2, we conclude that our results strongly support a contraction of d_{34} , as suggested by Andersen et al. [1].

The origin of the discrepancy in the two earlier LEED results in Table 1 is still not clear. Since these two experiments were at different temperatures (100 K [1] and 300 K [2]), one possibility is that it is related to a temperature dependence in the relaxation [2]. However, if there were a temperature effect, it would require an unusually large anharmonicity for such a low temperature, and it should normally have affected d_{12} and d_{23} as well. Furthermore, recent kinematic LEED results [3] and theoretical results [10] do not show significant

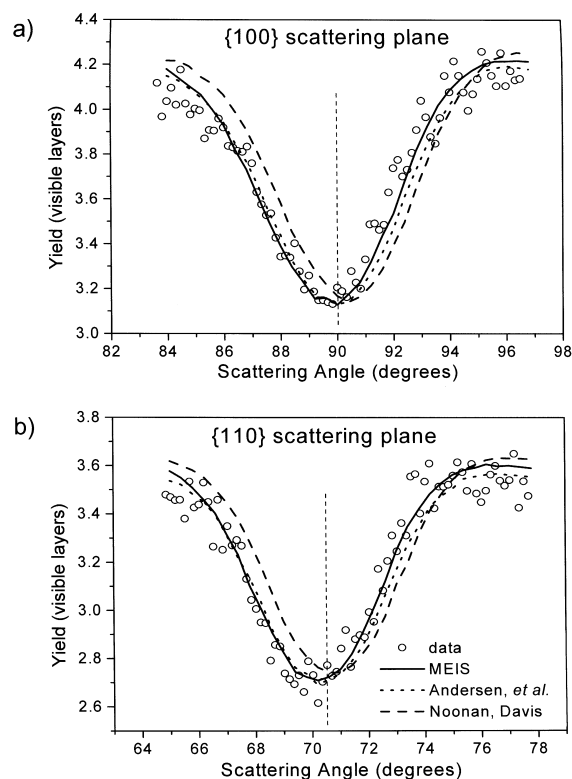


Fig. 2. Plot of MEIS blocking dips in the $\{100\}$ and $\{110\}$ scattering planes, together with the best-fit solution determined by ion-scattering simulation (solid line), the simulation result using the structure of Andersen et al. [1] (short dashes) and the simulation result using the structure of Noonan and Davis [2] (long dashes). The dashed vertical lines indicate the blocking dip positions for a bulk terminated surface.

thermal effects at low temperature. Therefore, it seems quite unlikely that this discrepancy was the result of the temperature difference. A second possibility could be that the accuracy of both analyses is not as good as quoted [2]. In the work of Noonan and Davis, the effect of including the d_{34} relaxation on eight different LEED beams using two different R -factors is reported. It was found that, for each R -factor, seven out of eight of the beams analyzed had a reduction in the R -factor when an expansion of d_{34} (with other structural parameters fixed) was used, significantly supporting the reported expansion. Such a detailed analysis on the effect of including d_{34} relaxation on the single-beam R -factors was not given in the

work of Andersen et al. However, their procedure for determining the best structure and errors is reported in detail, supplying strong support for their solution as well. The excellent agreement between the two studies on the first two layer spacings is also evidence that the technique is reproducible and that the accuracy claims are legitimate. A third possibility is the issue of sample preparation. The difficulty in preparing a good Al(110) surface with a sharp (1×1) LEED pattern is well known. Both groups report seeing slightly broadened spots. We also see the appearance of faint streaking along the [100] direction in LEED on our crystal after many cleaning cycles, as well as an attenuation of the scattered ion flux at low exit angles. These observations indicate the presence of imperfections on these surfaces. Although the effect of these imperfections on the outcome of either MEIS or LEED analyses is not clear, it seems unlikely that at low temperature they could be simulated by changes in layer spacings.

From Table 1 we can see that the four independent experiments give excellent agreement on the first two interlayer spacings. This in turn provides a dependable result useful for testing theories. A good match so far comes from the recent work of Marzari et al. [9,10] using Ensemble Density Functional Theory Molecular Dynamics.

By using medium-energy ion scattering in the channeling and blocking configuration, the room-temperature multilayer relaxation of Al(110) was investigated to help resolve a discrepancy occurring between two previous independent LEED results on the sign of the third-to-fourth interlayer spacing. Our results strongly favor a contraction in d_{34} , consistent with two other LEED results, and many other theoretical results. With this work, the experimental base for the interlayer structure has been extended to Al(110).

Acknowledgements

The authors would like to acknowledge the support of this work by the National Science Foundation through Grant No. DMR-9705367. We thank Richard Smith for providing the Al(110) crystal, and Nicola Marzari for valuable discussions.

References

- [1] J.N. Andersen, H.B. Nielsen, L. Petersen, D.L. Adams, *J. Phys. C* 17 (1984) 173.
- [2] J.R. Noonan, H.L. Davis, *Phys. Rev. B* 29 (1984) 4349.
- [3] H. Göbel, P. von Blanckenhagen, *Phys. Rev. B* 47 (1993) 2378.
- [4] R.N. Barnett, U. Landman, C.L. Cleveland, *Phys. Rev. B* 28 (1983) 1685.
- [5] K.M. Ho, K.P. Bohnen, *Phys. Rev. B* 32 (1985) 3446.
- [6] A.G. Eguluz, *Phys. Rev. B* 35 (1987) 5473.
- [7] T. Ning, Q. Yu, Y. Ye, *Surf. Sci.* 206 (1988) L857.
- [8] S.P. Chen, D.J. Srolovitz, A.F. Voter, *J. Mater. Res.* 4 (1989) 62.
- [9] N. Marzari, D. Vanderbilt, M.C. Payne, *Phys. Rev. Lett.* 79 (1997) 1337.
- [10] N. Marzari, D. Vanderbilt, A. De Vita, M.C. Payne, *Phys. Rev. Lett.*, in press.
- [11] J.F. van der Veen, *Surf. Sci. Rep.* 5 (1985) 199.
- [12] W.C. Turkenburg, W. Soszka, F.W. Saris, H.H. Kersten, B.G. Colenbrander, *Nucl. Inst. Meth.* 132 (1976) 587.
- [13] D.S. Gemmell, *Rev. Mod. Phys.* 46 (1974) 129.
- [14] J.W.M. Frenken, R.M. Tromp, J.F. van der Veen, *Nucl. Inst. Meth. Phys. Res. B* 17 (1986) 334.
- [15] R.M. Tromp, J.F. van der Veen, *Surf. Sci.* 133 (1983) 159.
- [16] I. Stensgaard, R. Feidenhans'l, J.E. Sørensen, *Surf. Sci.* 128 (1983) 281.
- [17] R.M. Tromp, M. Copel, M.C. Reuter, M.H. von Hoegen, J. Speidell, R. Koudijs, *Rev. Sci. Instrum.* 62 (1991) 2679.
- [18] L.C. Feldman, J.W. Mayer, *Fundamentals of Surface and Thin Film Analysis*, Pentice-Hall, Englewood Cliffs, NJ, 1986.